Pergamon

Int. J. Heat Mass Transfer. Vol. 39, No. 16, pp. 3311–3323, 1996

0017-9310/96 $15.00 + 0.00

PII: S0017-9310(96)00038-5

Low dimensional modeling of flow reactors

H. M. PARK and D. H. CHO

Department of Chemical Engineering, Sogang University, Seoul, Korea

(*Received* 12 *October* 1995 *and in final form* 19 *January* 1996)

Abstract—A new method is devised to obtain a low dimensional dynamic model of flow reactors governed by nonlinear partial differential equations. This is based on the Karhunen–Loève decomposition which is a technique of obtaining empirical eigenfunctions from the experimental or numerical data of a system. These empirical eigenfunctions are then employed as a basis set of a Galerkin procedure to reduce the distributed parameter system to a lumped parameter system in the optimal way in the sense that the degree of freedom of the resulting lumped parameter system is minimum. Flow reactors such as combustors, incinerators and CVD reactors cannot be described appropriately by conventional assumptions such as well-mixed flow or plug flow, and we need accurate flow patterns and convection–conduction/diffusion rates before characterizing or predicting their performance. Because the governing equations of these processes are nonlinear partial differential equations and, moreover, most practical flow reactors are of irregular shapes, the traditional Galerkin methods or orthogonal collocation are never feasible to lump these systems for the purpose of control or parameter estimation. But the Karhunen-Loève Galerkin procedure suggested in the present paper can easily reduce these nonlinear partial differential equations defined on irregular domains into reliable dynamic models with a few degrees of freedom, which may later be employed in the parameter estimation or reactor control. Copyright © 1996 Elsevier Science Ltd.

1. INTRODUCTION

In recent years there has been an increased emphasis on the study of flow reactors. A flow reactor is an empty vessel through which reactants pass to undergo various chemical reactions. Sometimes a catalyst is coated on the inner wall to facilitate chemical reaction or induce deposition of products. Examples of flow reactors are various combustors, internal combustion engines, incinerators for the treatment of toxic materials and chemical vapor deposition (CVD) reactors for the manufacturing of semiconductor chips. These flow reactors distinguish themselves from idealized simple reactors [1] such as continuously stirred tank reactors or plug flow reactors, in the sense that flow patterns must be accurately taken into consideration before predicting their performance appropriately. The flow patterns in most industrial flow reactors, especially at high Reynolds numbers, have recirculation zones and can be approximated neither by perfectly mixed flow nor one-dimensional plug flow. Because mixing of chemical species and heat transfer rate depend crucially on fluid flow, a reliable model of flow reactors must include detailed flow patterns. If accurate flow patterns are available, the temperature and concentration distributions are obtained by solving the convection-conduction and convection–diffusion equation, respectively. In principle, these flow patterns can be calculated by the solution of the Navier–Stokes equations using numerical techniques such as the finite volume method [2]. The resulting flow fields are reliable not only for laminar flows, but also for turbulent flows, as long as appropriate turbulence models are employed.

The real difficulty in the design and operation of flow reactors rests on appropriate dynamic modeling of the system for the purpose of control, parameter estimation and optimization. Even though we assume a steady flow field, the governing equations for heat and mass transfers are usually nonlinear distributed parameter systems defined on complicated domains. But it is not easy to get practical dynamic models of distributed parameter systems which can be implemented without undue complications, even for linear distributed parameter systems [3]. The degree of freedom of distributed parameter systems is essentially infinite and the relevant mathematical theory is too complicated to be implemented in industry. Moreover a satisfactory mathematical theory of nonlinear distributed parameter system is still lacking. Due to these difficulties many engineers rely on lumping techniques to model distributed parameter systems. These techniques reduce a distributed parameter system to a lumped parameter system with a finite number of degrees of freedom by using eigenfunctions of the system. The resulting lumped parameter systems may be used in control, or parameter estimation of the original distributed parameter systems rather easily with the help of relatively well advanced mathematical techniques for the former. Typical examples of these lumping techniques are Galerkin procedure and orthogonal collocation. But the eigenfunctions of a given system must be secured before applying these methods, so the applicability

NOMENCLATURE

a_i spectral coefficient premultiplying the jth eigenfunction when the concentration field is represented as a linear combination of eigenfunctions
D_A mass diffusivity
D_A^{ref} reference value of mass diffusivity
E activation energy
E^{ref} reference value of activation energy
f inlet temperature
$\mathbf{H}_{ji}$ matrix defined in equation (32c)
I maximum index number in the x-direction
k chemical reaction rate constant
k_{ro} frequency factor
k_{ro}^{ref} reference value of frequency factor
K maximum index number in the z-direction
K_{ij} two point correlation tensor of snapshots; equation (6)
$\mathbf{M}_j$ vector defined in equation (32a)
N number of snapshots employed in the Karhunen–Loève decomposition
$\mathbf{N}_{ji}$ matrix defined in equation (32d)
P pressure
$\mathbf{Q}_{ji}$ matrix defined in equation (32b)
R gas constant
$\mathbf{S}_j$ vector defined in equation (32e)
t time [s]
T temperature field
T_{avg} average value of temperature (= 750)
T^h temperature field with homogeneous boundary conditions
T^I temperature field with inhomogeneous boundary conditions
u x-component of the velocity vector $\mathbf{v}$
$\mathbf{v}$ velocity vector
v_n snapshots from a dynamic system
w z-component of the velocity vector $\mathbf{v}$
w_A concentration (mass fraction) of the species A
w_A^h concentration field with homogeneous boundary conditons
w_A^I concentration field with inhomogeneous boundary conditions.

Greek symbols

α inlet concentration (mass fraction)
$\boldsymbol{\alpha}_k$ eigenvector; equation (10)
κ thermal diffusivity
κ^{ref} reference value of thermal diffusivity
λ_k kth eigenvalue
μ viscosity
ρ density
ϕ_k kth empirical eigenfunction of concentration
φ_k kth empirical eigenfunction of temperature
Ω system domain.

Superscripts

0 initial value
ref reference value
T transpose.

Subscripts

avg average value
exact exact solution obtained by means of finite difference methods
i index in the x-direction
k index in the z-direction
KLG solution obtained by means of the Karhunen–Loève Galerkin procedure.

of these conventional techniques is limited to linear distributed parameter systems defined on regular domains (separable domains). Still another method is required to lump the distributed parameter systems defined on irregular domains. For the control and parameter estimation of these distributed parameter systems of the complex domain such as the flow reactors under consideration, we may reduce the original system of infinite degrees of freedom to one with a finite degree of freedom by discretizing it with the help of finite difference methods or finite element methods, but the resulting number of degrees of freedom is far larger than that of the Galerkin procedure or orthogonal collocation, rendering the resulting lumped parameter system inapplicable in industry. Recently, new control strategies such as model predictive control [4] have been devised to overcome these difficulties, but they are essentially empirical models based on the input and output of a given system and may become unstable as the set point (operating condition) of the system changes, thus requiring the design of a new model whenever the operation condition varies. Although the technique of model predictive control has the merit of small degrees of freedom, it has limitation in robustness because it is based on empirical relations. Moreover, the governing equation itself is never exploited in this kind of technique, losing much of the important physical information that we have already secured about the given distributed parameter system.

In the present work we examine the feasibility and efficiency of the Karhunen-Loève decomposition technique [5, 6] in the low dimensional modeling of flow reactors, with the eventual purpose of applying this low dimensional model to the control and parameter estimation. The Karhunen-Loève decomposition (K–L decomposition) is a technique enabling a stochastic field to be represented with a minimum degree of freedom [7, 8]. If the Karhunen–Loève decomposition is applied to a given stochastic field, we get a set of empirical eigenfunctions. When we want to reproduce that stochastic field with a certain criterion of accuracy—it can be represented with a minimum degree of freedom when employing these empirical eigenfunctions [9, 10]. The Galerkin procedure employing these empirical eigenfunctions as a basis set easily reduces the linear or nonlinear distributed parameter systems to lumped parameter systems with a small number of degrees of freedom, and its applicability is not limited, regardless of the geometric complexity of the system. Moreover, contrary to techniques such as model predictive control, this technique is not based on the empirical input–output relation of the system, but uses the governing equations exactly, thus yielding a dynamic model with sufficient robustness not affected by the changes in operating conditions.

In the present paper, we shall introduce the Karhunen-Loève decomposition, and then apply it to a flow reactor of irregular shape to get empirical eigenfunctions that most efficiently represent the system. This set of empirical eigenfunctions is used as a basis function of Galerkin procedure to lump the convection–conduction or convection–diffusion equations with chemical reaction. The resulting lumped parameter model is used to obtain temperature and concentration distribution of the system when the inlet temperature or concentration changes randomly, and then these temperature and concentration fields are compared with the exact results obtained by a finite difference solution of the original governing equations to demonstrate the efficiency and accuracy of the Galerkin procedure employing the empirical eigenfunctions of the Karhunen-Loève decomposition. This whole procedure or technique may be called Karhunen–Loève Galerkin procedure, in abbreviation, K–L Galerkin procedure. The K–L Galerkin technique can be applied to the control and parameter estimation of many other partial differential equations such as Navier–Stokes equation, as well as the convection–conduction equation treated in the present work.

2. THEORY

In this section, we explain the Karhunen–Loève decomposition and its applicability to the control and parameter estimation of distributed parameter systems. As an example of distributed parameter systems a flow reactor of irregular shape is considered. The governing equations of this system are the convection–conduction equation and the convection–diffusion equation with chemical reaction.

2.1. *The Karhunen–Loève decomposition*

To make this paper self-contained, we introduce the essence of the Karhunen–Loève decomposition. The Karhunen–Loève decomposition, expressed briefly, is a method of representing a stochastic field with a minimum number of degrees of freedom [5]. As a means of explaining the Karhunen–Loève decomposition we select N arbitrary irregularly shaped functions with $n = 1, 2, \ldots, N$. From now on, we call the irregular shapes of these functions $\{v_n\}$ 'snapshots'. The issue is how to obtain the most typical or characteristic structure $\phi(x)$ among these snapshots $\{v_n\}$. To make the mathematical development brief, the following notations are introduced:

$$v_n(x, y) \quad \text{a function defined in a function space} \tag{1}$$

$$\{v_n\} \quad \text{ensemble of snapshots} \tag{2}$$

$$(f, g) \equiv \int_\Omega f(x) g(x)\, d\Omega$$

$$\text{inner product in the function space} \tag{3}$$

$$\langle v_n \rangle \equiv \frac{1}{N} \sum_{n=1}^{N} v_n(x) \quad \text{ensemble average of snapshots.} \tag{4}$$

Then our objective is equivalently expressed so as to find a function $\phi(x)$ such that

$$\text{maximize} \quad \lambda = \frac{\langle (\phi, v_n)^2 \rangle}{(\phi, \phi)}. \tag{5}$$

We introduce the two point correlation function defined as,

$$K(x, x') = \langle v_n(x) v_n(x') \rangle = \frac{1}{N} \sum_{n=1}^{N} v_n(x) v_n^{\mathrm{T}}(x'). \tag{6}$$

It can be shown that the maximization problem of equation (5) is reduced to the following eigenvalue problem of the integral equation (7) [10]:

$$\int_\Omega K(x, x') \phi(x')\, dx' = \lambda \phi(x). \tag{7}$$

Namely, the function that maximizes λ of the equation (5) is equivalent to the eigenfunction of equation (7) with the largest eigenvalue. Usually this kind of integral equation can be solved by means of Schmidt–Hilbert technique or method of snapshot [6]. We assume the eigenfunction $\phi(x)$, a linear combination of snapshots as follows:

$$\phi(x) = \sum_k \alpha_k v_k(x). \tag{8}$$

Substituting this into equation (7) yields

$$\int_\Omega \frac{1}{N} \sum_{n=1}^{N} v_n(x) v_n^{\mathrm{T}}(x') \sum_k \alpha_k v_k(x') \, \mathrm{d}x' = \lambda \sum_n \alpha_n v_n(x) \tag{9}$$

Equation (9) may be expressed in the following form of a matrix eigenvalue problem:

$$\mathbf{C}_{nk}\boldsymbol{\alpha}_k = \lambda \alpha_n, \tag{10}$$

where

$$\mathbf{C}_{nk} \equiv \frac{1}{N} \int_\Omega v_n^{\mathrm{T}}(x') v_k(x') \, \mathrm{d}x'. \tag{11}$$

The above matrix $\mathbf{C}_{nk}$ is symmetric and positive definite. The eigenvector of the matrix eigenvalue problem, equation (10), is then substituted into equation (8) to generate the empirical eigenfunctions ϕ. Let's express the eigenvalues, $\lambda_1 > \lambda_2 > \ldots > \lambda_N$ and the corresponding eigenfunctions $\phi_1, \phi_2, \ldots, \phi_i$ in the order of magnitude of the eigenvalues. The eigenfunction ϕ_1 corresponding to the largest eigenvalue λ_1 is the most typical structure of the members of the snapshots $\{v_n\}$ and the eigenfunction ϕ_2 with the next largest eigenvalue λ_2 is the next typical structure, and so forth.

These empirical eigenfunctions ϕ can represent the system in the most efficient way [7, 8], and when employed as the basis functions of a Galerkin procedure [10, 11] the system can be represented with the minimum number of degrees of freedom.

2.2. *The system and governing equations*

The governing equations of a two-dimensional planar flow reactor of unit length with irregular boundaries shown in Fig. 1 are used to demonstrate the Karhunen–Loève Galerkin procedure. The boundary denotes the centerline of the symmetry. The flow field, which is assumed to be steady, is obtained by solving the following incompressible Navier–Stokes equation:

$$\rho\left(u\frac{\partial u}{\partial x} + w\frac{\partial u}{\partial z}\right) = -\frac{\partial P}{\partial x} + \mu\left(\frac{\partial^2}{\partial x^2} + \frac{\partial^2}{\partial z^2}\right)u \tag{12}$$

$$\rho\left(u\frac{\partial w}{\partial x} + w\frac{\partial w}{\partial z}\right) = -\frac{\partial P}{\partial z} + \mu\left(\frac{\partial^2}{\partial x^2} + \frac{\partial^2}{\partial z^2}\right)w \tag{13}$$

$$\frac{\partial u}{\partial x} + \frac{\partial w}{\partial z} = 0, \tag{14}$$

where u and w are the x- and z- component of the velocity field $\mathbf{v}$, P the pressure, ρ the density, and μ the viscosity. The relevant boundary conditions are as follows:

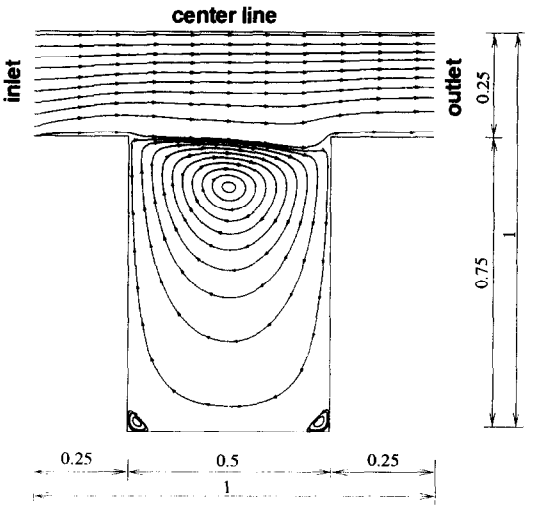

Fig. 1. System under consideration. Only the lower part below the symmetric line is shown. The temperature and concentration fields have Neumann boundary conditions at the wall. Either the inlet temperature or the inlet concentration is changed to control the outlet concentration. The streamlines are obtained for the case of $Re = 100$ at steady state.

$$\text{inlet} \quad u = U(=100) \quad w = 0 \tag{15}$$

$$\text{center line} \quad \frac{\partial u}{\partial z} = 0 \quad w = 0 \tag{16}$$

$$\text{outlet} \quad \frac{\partial u}{\partial x} = 0 \quad \frac{\partial w}{\partial x} = 0 \tag{17}$$

$$\text{all other boundaries} \quad u = w = 0. \tag{18}$$

The SIMPLE algorithm of Patankar [2] is employed to obtain a steady-state flow field at the Reynolds number of 100, when the length scale is the length of the reactor, l. The streamline of this flow field is also shown in Fig. 1 when 82×82 grids are employed. Using this flow field we now concentrate on the convection–diffusion–reaction of a reactant A. Let's assume that the reactant A decays according to the following first-order reaction:

$$A \xrightarrow[k]{} B, k = k_{\mathrm{ro}} \mathrm{e}^{-E/RT} \tag{19}$$

where, k is the reaction constant, k_{ro} the frequency factor, E the activation energy and R the gas constant. The governing equations of the temperature and concentration fields are the following convection–conduction and convection–diffusion equations with a source term due to chemical reaction. We neglect heat generation arising from the chemical reaction.

$$\frac{\partial T}{\partial t} + \nabla \cdot T\mathbf{v} = \kappa \nabla^2 T \tag{20}$$

$$\frac{\partial w_{\mathrm{A}}}{\partial t} + \nabla \cdot w_{\mathrm{A}}\mathbf{v} = D_{\mathrm{A}} \nabla^2 w_{\mathrm{A}} - k_{\mathrm{ro}} \mathrm{e}^{-E/RT} w_{\mathrm{A}}, \tag{21}$$

where T is the temperature field, w_A is the concentration (mass fraction) of the species A, κ the thermal diffusivity and D_A the mass diffusivity. The boundary conditions for T and w_A are given as,

$$\text{inlet} \quad T = T_{in} \quad w_A = w_{A,in} \tag{22}$$

$$\text{centerline} \quad \frac{\partial T}{\partial z} = 0 \quad \frac{\partial w_A}{\partial z} = 0 \tag{23}$$

$$\text{outlet} \quad \frac{\partial T}{\partial x} = 0 \quad \frac{\partial w_A}{\partial x} = 0 \tag{24}$$

$$\text{all other boundaries} \quad \frac{\partial T}{\partial n} = 0 \quad \frac{\partial w_A}{\partial n} = 0, \tag{25}$$

where $\partial/\partial n$ denotes the normal derivative at the wall.

We shall change the outlet concentration of the reactant A by adjusting the inlet concentration of A (case A) or by adjusting the inlet temperature of the feed stream (case B). For both cases, the results from the dynamic models based on the Karhunen–Loève Galerkin method shall be compared with the exact results from the finite difference solution to assess the performance of the Karhunen–Loève Galerkin procedure.

2.2.1. *Case A : control of the outlet concentration by adjusting the inlet concentration.* In this subsection, we develop equations for the case where the inlet concentration is adjusted to control the outlet concentration. Since the temperature boundary condition at the wall is adiabatic, the temperature field assumes a constant value over the whole domain at the steady state if the heat of the reaction is neglected. Because the chemical species cannot penetrate through the reactor walls, the appropriate concentration boundary condition is also of Neumann type. The inlet mass fraction (concentration) of A is assumed to have an arbitrary value between 0.02 and 0.1. The concentration (mass fraction) is divided into two parts, w_A^I and w_A^h.

$$w_A = w_A^h + \alpha w_A^I, \tag{26}$$

where w_A^h satisfies the homogeneous boundary conditions and w_A^I satisfies the inhomogeneous boundary conditions, and α represents the inlet mass fraction. The w_A^I is forced to satisfy the following equation and boundary conditions:

$$\nabla \cdot w_A^I \mathbf{v} = D_A^{ref} \nabla^2 w_A^I - k_{ro}^{ref} e^{-E^{ref}/RT_{avg}} w_A^I \tag{27}$$

$$\text{inlet} \quad w_A^I = 1 \tag{28a}$$

$$\text{all other boundaries:} \quad \frac{\partial w_A^I}{\partial n} = 0, \tag{28b}$$

where D_A^{ref}, k_{ro}^{ref}, E^{ref}, T_{avg} are reference values to make the inhomogeneous solution w_A^I independent of D_A, k_{ro}, E, T of the system under consideration. With the steady-state flow field shown in Fig. 1, and with the values of D_A^{ref}, k_{ro}^{ref}, E^{ref} and T_{avg} being 1, 1000, 5000 and 750, respectively, the resulting inhomogeneous mass fraction field w_A^I is obtained using equations (27) and (28a, b). The governing equation for w_A^h is obtained by substituting equation (26) into equation (21) in the following form:

$$\frac{\partial w_A^h}{\partial t} + \nabla \cdot w_A^h \mathbf{v} = D_A \nabla^2 w_A^h + \alpha D_A \nabla^2 w_A^I - \alpha D_A^{ref} \nabla^2 w_A^I - k_{ro} e^{-E/RT} w_A^h - \alpha k_{ro} e^{-E/RT} w_A^I + \alpha k_{ro}^{ref} e^{-E^{ref}/RT_{avg}} w_A^I - w_A^I \frac{\partial \alpha}{\partial t}. \tag{29}$$

In equation (29), the temperature field is a constant (i.e. the inlet value) as mentioned previously. A set of w_A^h fields are obtained by solving equation (29), while imposing a step change on α from 0.02 to 0.1, and they are used as snapshots for the Karhunen–Loève decomposition to generate empirical eigenfunction ϕ_is. A Galerkin procedure employing these empirical eigenfunctions as a basis set is then applied to the present system of the convection–diffusion equation with chemical reaction defined on a complex domain to convert it to a small number of ordinary differential equations. In the beginning, we represent w_A^h as a linear combination of the empirical eigenfunctions

$$w_A^h = \sum_{i=1} a_i \phi_i \tag{30}$$

where the ϕ_is are indexed in the order of magnitude of the corresponding eigenvalues. Substituting equation (30) into equation (29) and applying the Galerkin procedure, we find

$$\mathbf{M}_j \frac{da_j}{dt} + \sum_i \mathbf{Q}_{ji} a_i + \sum_i \mathbf{H}_{ji} a_i + \sum_i \mathbf{N}_{ji} a_i = \mathbf{S}_j \tag{31}$$

where

$$\mathbf{M}_j = \int_\Omega \phi_j^2 \, d\Omega \tag{32a}$$

$$\mathbf{Q}_{ji} = \int_\Omega \phi_j \left(u \frac{\partial \phi_i}{\partial x} + w \frac{\partial \phi_i}{\partial z} \right) d\Omega \tag{32b}$$

$$\mathbf{H}_{ji} = D_A \int_\Omega \left(\frac{\partial \phi_j}{\partial x} \frac{\partial \phi_i}{\partial x} + \frac{\partial \phi_j}{\partial z} \frac{\partial \phi_i}{\partial z} \right) d\Omega \tag{32c}$$

$$\mathbf{N}_{ji} = k_{ro} \int_\Omega \phi_j \phi_i e^{-E/RT} \, d\Omega \tag{32d}$$

$$\mathbf{S}_j = \alpha \int_\Omega \phi_j [(D_A - D_A^{ref}) \nabla^2 w_A^I + (k_{ro}^{ref} e^{-E^{ref}/RT_{avg}} - k_{ro} e^{-E/RT}) w_A^I] \, d\Omega - \frac{d\alpha}{dt} \int_\Omega \phi_j w_A^I \, d\Omega. \tag{32e}$$

The set of ordinary differential equations, equation (31), may be solved by means of a fourth-order Runge–Kutta method [12]. Since this dynamic model of ordinary differential equations is obtained from the Galerkin procedure employing the empirical eigen-

functions (i.e. the Karhunen–Loève Galerkin procedure), the degree of freedom or the number of equations is usually very small.

2.2.2. *Case B: control of outlet concentration (mass fraction) by adjusting the inlet temperature.* On the contrary to the previous case (case A), we change the inlet temperature to adjust the reaction rate to control the outlet concentration in this subsection. For the case A of subsection 2.2.1, the temperature is a constant over the whole reactor, but in the present situation, the temperature field has spatial and temporal variations due to the inlet temperature changes. Both the temperature and concentration (mass fraction) fields can be predicted accurately by using the Karhunen–Loève Galerkin procedure as described in the sequel. The governing equation for the temperature field, equation (20), is treated in the Karhunen–Loève Galerkin procedure as follows. First, as before, we divide the temperature field T into two parts, T^{I} and T^{h}.

$$T = T^{\mathrm{h}} + fT^{\mathrm{I}}, \tag{33}$$

where T^{h} satisfies the homogeneous boundary conditions and T^{I} satisfies the inhomogeneous boundary conditions, and f denotes the inlet temperature. Then T^{I} is forced to satisfy the following equation and boundary conditions:

$$\nabla \cdot T^{\mathrm{I}}\mathbf{v} = \kappa^{\mathrm{ref}}\nabla^2 T^{\mathrm{I}} \tag{34}$$

$$\text{inlet} \quad T^{\mathrm{I}} = 1 \tag{35a}$$

$$\text{all other boundaries} \quad \frac{\partial T^{\mathrm{I}}}{\partial n} = 0. \tag{35b}$$

The solution of equations (34) and (35a, b) is easily found to be a uniform value of 1. The governing equation for T^{h} is then obtained by substituting equation (33) into equation (20) as follows:

$$\frac{\partial T^{\mathrm{h}}}{\partial t} + \nabla \cdot T^{\mathrm{h}}\mathbf{v} = f(\kappa - \kappa^{\mathrm{ref}})\nabla^2 T^{\mathrm{I}} + \kappa\nabla^2 T^{\mathrm{h}} - T^{\mathrm{I}}\frac{\partial f}{\partial t}. \tag{36}$$

The governing equations for the concentration field are the same as those presented in the previous subsection (case A), i.e. equations (26)–(29), except the $\partial\alpha/\partial t$ term disappear in equation (29) because the inlet concentration does not change in the present case (case B). After imposing a step change on the inlet temperature f from 500 to 1000, we solve equations (29) and (36) to obtain $w_{\mathrm{A}}^{\mathrm{h}}$ and T^{h} fields at appropriate time intervals, and use them as concentration and temperature snapshots, respectively. To each of these sets of snapshots, the Karhunen–Loève decomposition is applied to yield the concentration eigenfunctions ϕ_js and the temperature empirical eigenfunctions φ_js. These sets of empirical eigenfunctions are then employed as the basic sets of the Karhunen–Loève Galerkin procedure to reduce equations (29) and (36) into two sets of ordinary differential equations of a few degrees of freedom, which constitute the low dimensional dynamic model of the flow reactor for the case B.

3. RESULTS

In this section, we describe how to take snapshots from the solution of the convection–conduction and convection–diffusion equations considered in the present work, and investigate the properties of the empirical eigenfunctions obtained from the application of the Karhunen–Loève decomposition to these snapshots. Furthermore, the accuracy and efficiency of the low dimensional dynamic model obtained from the Galerkin procedure employing these empirical eigenfunctions as basis functions, are examined by comparing their solutions with those of finite difference method applied to the original convection–conduction and convection–diffusion equations with chemical reaction.

3.1. *Empirical eigenfunctions obtained from the Karhunen–Loève decomposition*

Before the empirical eigenfunctions from the Karhunen–Loève decomposition can be useful, the snapshots must be representative of the dynamic characteristics of the system under consideration. The dynamic model's aim is to predict exactly the temperature and concentration fields of the flow reactor when the inlet concentration or the inlet temperature changes randomly. Thus, the snapshots have been obtained in the following way. We shall explain this procedure in detail only for case A. Following almost the same procedure one can obtain snapshots and empirical eigenfunctions for case B. We take as an initial concentration distribution of $w_{\mathrm{A}}^{\mathrm{h}}$ the steady-state situation when the inlet concentration α is 0.02. Next, we increase the inlet concentration α to 0.1 and solve equation (29) to obtain the concentration distributions at an appropriate time interval until a new steady state is reached, and use these concentration distributions as snapshots of case A, i.e. the ensemble members. The temperature field has a constant value of 750 during this procedure. The range of α (i.e. $0.02 \sim 0.1$) is taken to be the same as that of the permissible inlet concentration of the actual system under consideration. Initially a concentration boundary layer with a steep concentration gradient appears near the inlet, and the concentration gradient becomes less steep as time goes on. Thus the frequency to take snapshots should be high initially and it may be decreased as time elapses to obtain a set of snapshots that fully characterize the concentration boundary layer formed during the process. The values of parameters adopted are those of the reference values, i.e. $D_{\mathrm{A}} = D_{\mathrm{A}}^{\mathrm{ref}} = 1$, $k_{\mathrm{ro}} = k_{\mathrm{ro}}^{\mathrm{ref}} = 1000$, $E = E^{\mathrm{ref}} = 5000$. At steady state the $w_{\mathrm{A}}^{\mathrm{h}}$ becomes zero over the whole domain. Table 1 indicates the moments when the snapshots are taken. The time intervals are chosen such that the snapshots must contain important

Table 1. Time interval and number of snapshots for case A and case B; e.g. for case A when we take 400 snapshots, 200 snapshots are obtained at the time interval 5×10^{-5} during time period 0.0000–1×10^{-2} s, and another 100 snapshots are obtained at the time interval of 1×10^{-4} during time period 1×10^{-2}–2×10^{-2}, and so forth

	Case A		Case B			
	Concentration		Temperature		Concentration	
Number	Time (s)	Time interval	Time (s)	Time interval	Time (s)	Time interval
100	0.0–5×10^{-3}	5×10^{-5}	0.0–1×10^{-2}	1×10^{-4}	0.0–2.5×10^{-2}	2.5×10^{-4}
100	5×10^{-3}–1×10^{-2}	5×10^{-5}	1×10^{-2}–4×10^{-2}	3×10^{-4}	2.5×10^{-2}–7.5×10^{-2}	5×10^{-4}
100	1×10^{-2}–2×10^{-2}	1×10^{-4}	4×10^{-2}–1×10^{-1}	6×10^{-4}	7.5×10^{-2}–2.0×10^{-1}	1.25×10^{-3}
100	2×10^{-2}–5×10^{-2}	3×10^{-4}	1×10^{-1}–5×10^{-1}	4×10^{-3}	2.0×10^{-1}–4.0×10^{-1}	2×10^{-3}

dynamic characteristics of the system, especially the formation and decay of the concentration boundary layer near the inlet. Table 1 says that when we take 400 snapshots, 200 of them are obtained at the time interval of 5×10^{-5} during $0.0000 \sim 0.0100$ s and an additional 100 snapshots are taken at the time interval of 1×10^{-4} during $0.0100 \sim 0.0200$ s, and so forth. Figure 2(a–d) shows some of these snapshots at the time indicated. At $t = 5 \times 10^{-4}$ we can observe the development of a concentration boundary layer due to the rapid change of concentration at the inlet, and as time goes on the concentration gradient near the inlet becomes less steep and eventually the concentration field approaches the steady-state value of zero. We can also observe the movement of a concentration wave near the inlet.

The Karhunen–Loève decomposition is then applied to these snapshots to yield empirical eigenfunctions. Figure 3(a–d) depicts the first, second, seventh and eighth eigenfunction in the order of magnitude of the corresponding eigenvalues when 400 snapshots have been adopted. Among the four eigenfunctions shown in Fig. 3, the eigenfunctions with large eigenvalues [Fig. 3(a, b)] take the shape of smooth, large scales that are typical structures among members of the snapshots. These two eigenfunctions

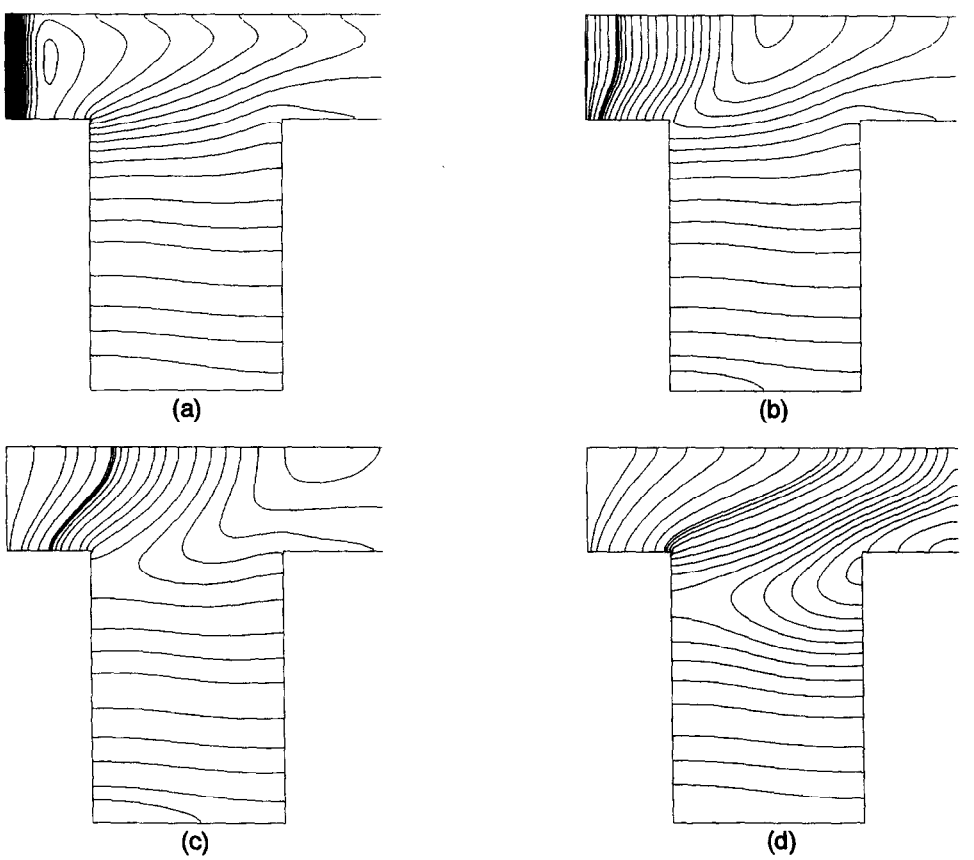

Fig. 2. The snapshots (concentration field w_A^h with homogeneous boundary conditions) at various time instants; (a), (b), (c) and (d) correspond to 5×10^{-4}, 5×10^{-3}, 1×10^{-2} and 2×10^{-2} s, respectively.

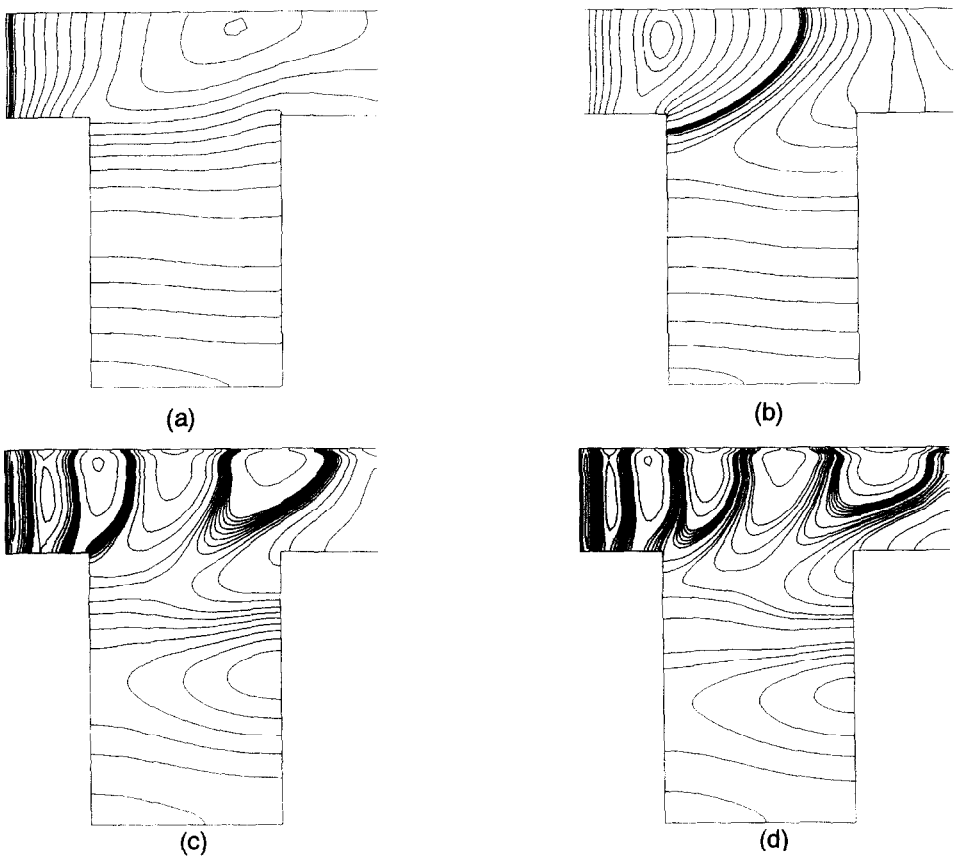

Fig. 3. Dominant eigenfunctions (case A) obtained from 400 snapshots of Table 1. (a) Normalized eigenvalue = 0.88755, (b) normalized eigenvalue = 8.2568×10^{-2}, (c) normalized eigenvalue = 4.4789×10^{-4}, (d) normalized eigenvalue = 1.8245×10^{-4}.

can also represent the moving concentration wave near the inlet region. But as the magnitude of eigenvalue decreases, the corresponding empirical eigenfunctions have a tendency to have small scale shapes. In other words, the empirical eigenfunctions with large eigenvalues represent the global concentration distribution of the system and the distinguished characteristic of the moving concentration wave, and empirical eigenfunctions of smaller eigenvalues represent concentration boundary layer caused by the rapid concentration change near the inlet and other small scale shapes not captured by eigenfunctions of large eigenvalues.

We may almost follow the same procedure to obtain empirical eigenfunctions for temperature and concentration fields for case B. Also indicated in Table 1 are the instants when the temperature and concentration snapshots are taken in case B.

3.2. *The dynamic model based on the Karhunen–Loève Galerkin (K–L Galerkin) method*

To investigate the accuracy of the dynamic models for case A and case B, we examine the cases where the inlet concentration α experiences a random change between 0.02 and 0.1 for case A, and the inlet temperature f experiences a random change between 500 and 1000 for case B, respectively. This can serve as a preliminary step toward the application of the present dynamic models to real control problems. The dynamic models for case A and case B have been constructed by applying a Galerkin procedure to equation (29) employing 15 concentration eigenfunctions (case A), and to equation (29) (with $\partial\alpha/\partial t = 0$) and equation (36) with 15 concentration and 15 temperature eigenfunctions (case B), respectively. Afterwards, if not mentioned otherwise, it will be assumed that we employ the empirical eigenfunctions obtained from the 400 snapshots of Table 1.

3.2.1. *Randomly changing inlet concentration (case A) or inlet temperature (case B).* In this subsection we consider the case where the inlet concentration α (case A) or the inlet temperature f (case B) changes randomly.

The low dimensional dynamic model for the case A, equation (31), has been solved when the inlet concentration α changes randomly between 0.02 and 0.1 at every 0.001 s (i.e. every 20 integration time steps Δt) and is compared with the exact solution using a finite difference method. Figure 4 shows the random variation of the inlet concentration α constructed by a random number generation code. The results are

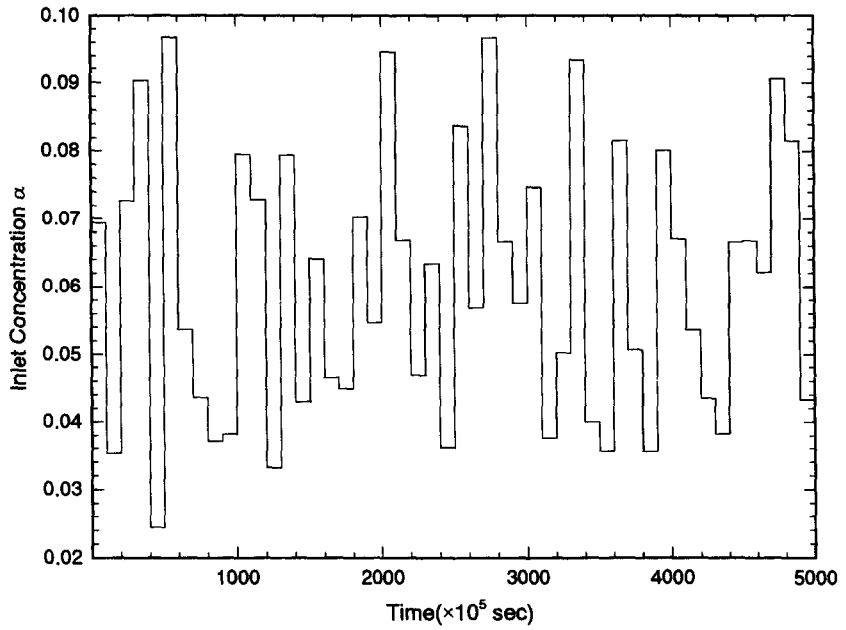

Fig. 4. The random variation of the inlet concentration α between 0.02 and 0.1.

presented in Fig. 5 where concentration obtained both from the dynamic model [equation (31)] and from the original equation [equation (29)] are shown at various locations in the flow reactor. In Fig. 5, the solid lines indicate the solution from the dynamic model of Karhunen–Loève Galerkin procedure and the dashed lines from the finite difference method. Since the initial value of the inlet concentration α is 0.02 and the time-varying α is always larger than or equal to 0.02, the concentration in the flow reactor starts to increase globally as time goes on. Figure 5 shows this gradual increase of concentration. Since location 1 in Fig. 5 is nearer to the inlet than location 3, the concentration rise at location 1 is finished at an earlier stage and reaches stationary state, where the concentration at that same point follows the fluctuation of the inlet concentration α. In Fig. 5, the exact solution by the finite difference method and the solution from the dynamic model of the Karhunen–Loève Galerkin procedure are almost the same.

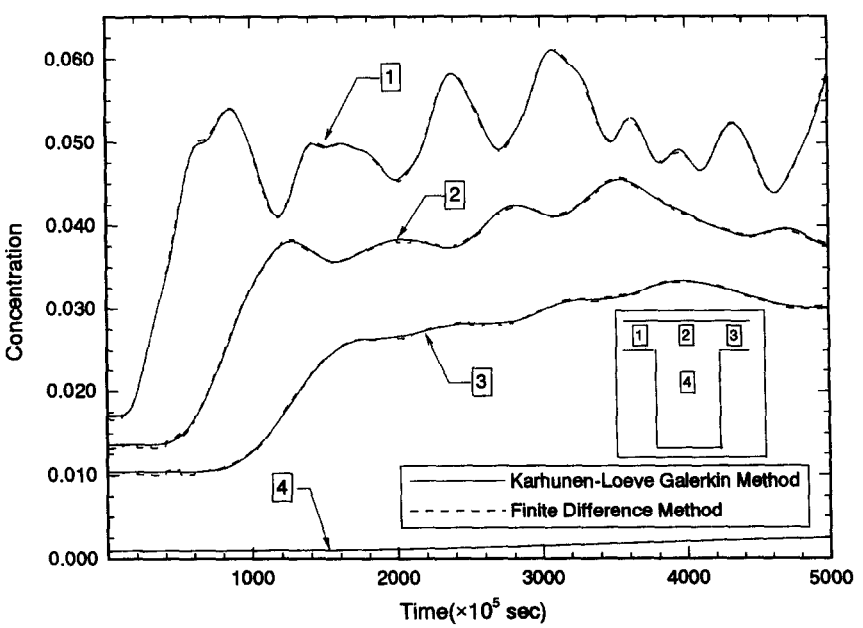

Fig. 5. The temporal variations of concentration at selected points for the case A when α changes randomly (cf. Fig. 4). Solid lines (——) are solutions from the Karhunen–Loève Galerkin procedure and dashed lines (– – –) are exact solutions from the finite difference method.

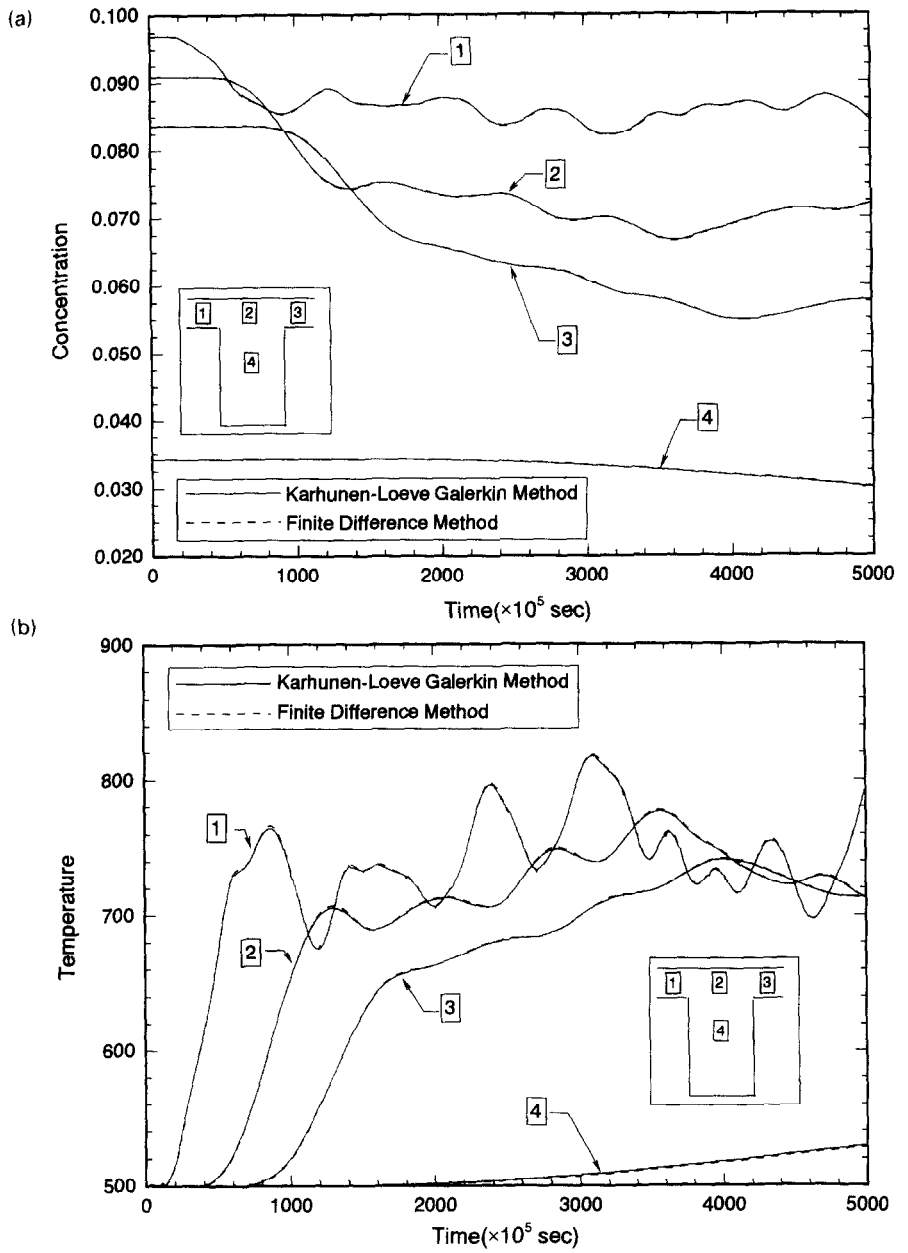

Fig. 6. The temporal variations of concentration and temperature at selected points for the case B when f changes randomly between 500 and 1000 K, (a) concentration (b) temperature.

Similarly, the dynamic model for case B is solved by a fourth-order Runge–Kutta method when the inlet temperature f is changing randomly between 500 and 1000 K, and in Fig. 6(a, b) the resulting concentration and temperature at selected points are presented and compared with exact values obtained by solving the original partial differential equations (29) and (36). In this case, the error is almost negligible, as in case A.

This result is one clear demonstration that the Karhunen–Loève Galerkin procedure can efficiently reduce partial differential equations defined on complex geometries to dynamic models of a small degree of freedom, and the resulting low dimensional models can simulate the real systems with almost the same accuracy as the original partial differential equations. Moreover, the Karhunen–Loève Galerkin method explained in the present paper can be applied to many other formidable nonlinear partial differential equations in engineering and science, such as the Navier–Stokes equations, and these results shall be published as a separate paper later.

3.2.2. *The effect of values of system parameters.* In this section, we investigate whether a dynamic model, made of empirical eigenfunctions based on snapshots taken with a reference set of parameter values (i.e. $D_A = 1.0$, $k_{ro} = 1000$, $E = 5000$), can be applied to

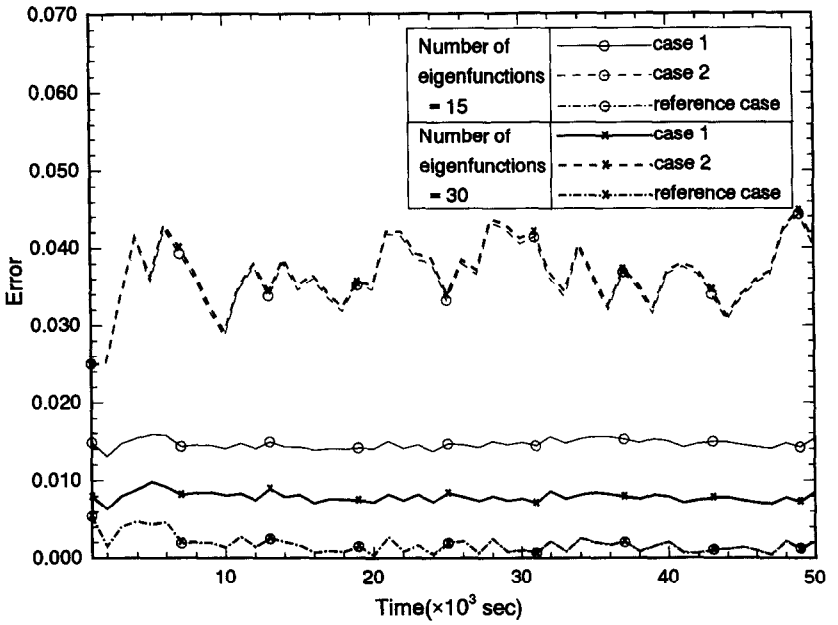

Fig. 7. The temporal variation of errors of the reference dynamic model with respect to a random change of the inlet concentration when it is applied to systems with widely different values of parameters.

cases of different sets of these parameter values. For convenience of communication, we call this dynamic model, based on the reference set of parameter values, the reference dynamic model.

As a first illustration we chose case A, where we change the inlet concentration to control the outlet concentration, and apply the reference dynamic model to one case where the value of k_{ro} is 100 instead of the original value of 1000, while values of other parameters are kept the same (case 1), and to the other case where k_{ro} is 10000 and D_A is 10 while E is still 5000 (case 2). Figure 7 plots the results for both case 1 and case 2 when the reference dynamic model uses 15 and 30 empirical eigenfunctions, respectively. We define the error in the following manner:

$$\text{Error} = \sum_{i=1}^{I}\sum_{k=1}^{K} \frac{|w^h_{A,KLG}(i,k) - w^h_{A,exact}(i,k)|}{|w^h_{A,exact}(i,k)|} / (I \times K) \tag{37}$$

where I and K are the maximum grid numbers in the i and k direction, respectively, and $w^h_{A,KLG}$ denotes the solution by means of the K–L Galerkin method and $w^h_{A,exact}$ the finite difference solution of the original partial differential equation.

This figure shows that the reference dynamic model employing 15 eigenfunctions, though predicts accurate results for the reference set of parameter values with less than 0.5% error, yields poor predictions for case 1 and case 2 (i.e. 1.5 and 4% errors, respectively). When the number of empirical eigenfunctions employed in the reference dynamic model is increased from 15 to 30, the errors do not decrease, except case 1 whose value decreases from 1.5 to 0.8%. This implies that the eigenmodes of case 1 are very similar to those of the reference case, and it requires more eigenfunctions to resolve the concentration field of case 1 than the reference case, if the empirical eigenfunctions of the reference case are employed. But it is apparent that new eigenmodes different from those of the reference case appear in case 2 due to a complicated interaction of convection, diffusion and reaction in the flow reactor. Because these new eigenmodes cannot be represented as linear combinations of the empirical eigenfunctions of the reference case, the error of case 2 does not decrease even though we employ more eigenfunctions in the reference dynamic model. In the present paper, this difficulty is overcome as follows. We obtain three sets of 200 snapshots with parameter values of case 1, case 2 and the reference case, respectively. To these 600 snapshots, the Karhunen–Loève decomposition is applied to get a set of empirical eigenfunctions. These eigenfunctions are expected to resolve every important aspect of concentration fields of the case 1 and case 2 as well as the reference case, since they are based on the snapshots of case 1, case 2 and the reference case. In Fig. 8 are shown the errors of case 1, case 2 and the reference case when a dynamic model based on 30 empirical eigenfunctions from these combined snapshots are used. This figure shows that the maximum error which arises for the case 2 is less than 0.6%. This is in contrast with the results of Fig. 7, where the error of case 2 is about 4% when employing 30 eigenfunctions of the reference case. Thus, we may conclude that this low dimensional dynamic model based on the combined snapshots can simulate the governing equations of the flow reactor faithfully over the abovementioned range of parameter values, and consequently can be employed in the parameter estimation

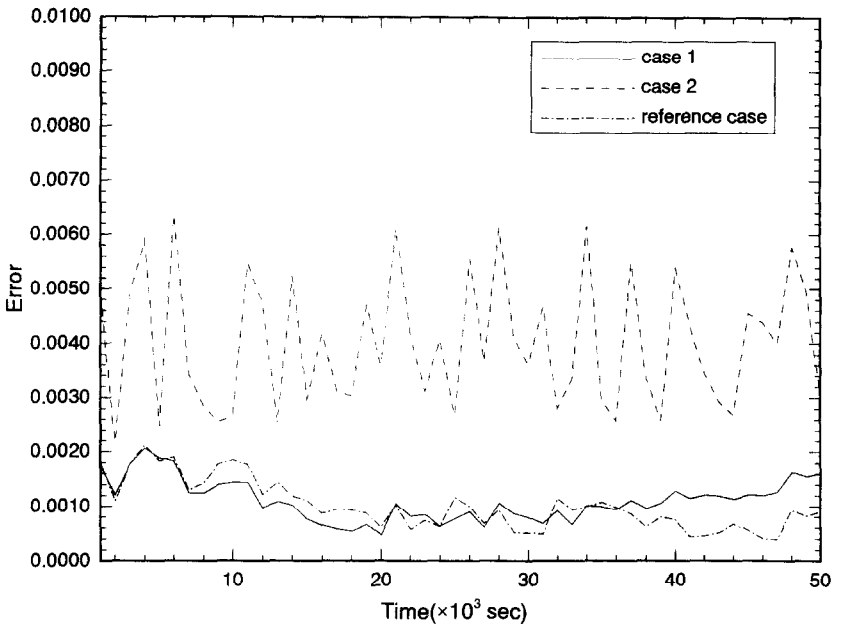

Fig. 8. The temporal variation of errors of the dynamic model based on the combined snapshots with respect to a random change of the inlet concentration when it is applied to systems with widely different values of parameters.

or identification if the parameter values to be estimated are within the same range. This also suggests a method of constructing low dimensional dynamic models by means of the Karhunen–Loève Galerkin procedure that are valid over a wide range of parameter values.

3.3. *Computational time of the Karhunen–Loève Galerkin procedure*

Until now we have described some details of the Karhunen–Loève Galerkin procedure, i.e. how to obtain appropriate snapshots, how to obtain efficient empirical eigenfunctions from these snapshots, how to construct low dimensional dynamic models by means of the K–L Galerkin procedure, and finally some results of the performance of these low dimensional dynamic models. From a numerical experiment we concluded that an 82×82 grid is sufficient for an accurate numerical solution of our governing convection–conduction equations [equations (29) and (36)] using the finite difference method. All the results of the present paper are thus based on numerical solution employing 82×82 grid points.

When problems of control and/or parameter estimation of distributed parameter systems of industrial applications are considered, it is very important to obtain low dimensional dynamic models before devising and implementing any practical control or parameter estimation schemes. The actual implementation of control or parameter estimation schemes requires repeated computations of dynamic models and one cannot expect on-line control or parameter estimation without faithful low dimensional dynamic models.

Now it may be interesting to consider the CPU time required for each step in the Karhunen–Loève Galerkin procedure, and compare the CPU time of the resulting low dimensional model from the Karhunen–Loève Galerkin procedure with that of the finite difference method when simulating the convection–conduction problem defined on a complex domain considered in the present work for a certain time period (say, 5 s). We investigate the CPU time requirement for the case A in this section. When Sparc 10 workstation is used, it requires 20 min 34 s to obtain 400 snapshots, 9 min 21 s to obtain empirical eigenfunctions from these snapshots, and 1 s to construct a low dimensional model of 15 degrees of freedom with these empirical eigenfunctions. Now, when the inlet concentration α is changing randomly as depicted in Fig. 4, it requires only 6 s to simulate this system during 5 s when the low dimensional model of 15 degrees of freedom from the K–L Galerkin procedure is employed, which is contrasted with 3037 min 30 s required when a finite difference method is employed. This drastic reduction in computation time will facilitate the implementation of many control schemes on distributed parameter systems of industrial applications.

4. CONCLUSION

Sets of empirical eigenfunctions, that represent the dynamics of convection–conduction or convection–diffusion equations with chemical reactions defined on a two-dimensional complicated geometry efficiently, are obtained by means of the Karhunen–Loève decomposition, and a Galerkin procedure

employing these empirical eigenfunctions (the Karhunen–Loève Galerkin method) is used to reduce the partial differential equations to a small number of ordinary differential equations. The resulting set of ordinary differential equations, when compared with the original governing equations expressed as partial differential equations, could describe the system almost exactly. This technique of the Karhunen–Loève Galerkin procedure can be applied not only to the convection–conduction type equations of the present work, but also to other general partial differential equations (distributed parameter systems) that cannot be treated by the traditional Galerkin methods or orthogonal collocation due to the geometric complexity or nonlinearity.

One of the most important steps in the Karhunen–Loève Galerkin procedure is how to obtain appropriate snapshots. The snapshots must include informations about the dynamic characteristics of the system in order to yield empirical eigenfunctions that will represent the dynamics of the system faithfully. When the inlet concentration or temperature of the flow reactors changes as in our present work, the snapshots must include informations about the formation and decay of the concentration or thermal boundary layer in order to obtain efficient empirical eigenfunctions through the Karhunen–Loève decomposition technique. Only the dynamic model based on these empirical eigenfunctions that contain informations about the formation and decay of the concentration or thermal boundary layer will be able to simulate the system faithfully. On the condition that the same snapshots are used to yield empirical eigenfunctions, the accuracy of the dynamic model improves as the number of empirical eigenfunctions employed in the K–L Galerkin procedure increases. Especially when the inlet concentration or temperature of the system changes continuously, the concentration of thermal boundary layer always exists, and only dynamic models including many empirical eigenfunctions with small eigenvalues produce accurate results in this case.

When a reference dynamic model which is based on reference values of the parameters is applied to the same flow reactor with widely different values of parameters, it may be difficult to yield accurate predictions due to the new eigenmodes generated by a complicated interaction of convection, diffusion and reaction. In the present paper, this difficulty is overcome by combining various sets of snapshots with widely different values of parameters to construct eigenfunctions. The low dimension dynamic model based on these eigenfunctions is shown to simulate the system over a wide range of parameter space and may be employed in the parameter estimation or identification.

In conclusion, as explained in the present paper, the Karhunen–Loève Galerkin procedure that employs empirical eigenfunctions from the Karhunen–Loève decomposition easily reduces linear or nonlinear partial differential equations defined on complex geometries to dynamic models with a small degree of freedom. This technique can be applied not only to the convection–conduction type equations of the present work, but also to more complicated partial differential systems such as Navier–Stokes equations for the purpose of parameter estimation or system control.

REFERENCES

1. O. Levenspiel, *Chemical Reaction Engineering* (2nd Edn). Wiley, New York (1972).
2. S. V. Patankar, *Numerical Heat Transfer and Fluid Flow*. McGraw Hill, New York (1980).
3. W. H. Ray and D. G. Lainiotis, *Distributed Parameter Systems*. Marcel Dekker, New York (1978).
4. T. Söderström and P. Stoica, *System Identification*. Prentice Hall, Englewood Cliffs, NJ (1989).
5. M. Loève, *Probability Theory*. Van Nostrand, Princeton, NJ (1955).
6. L. Sirovich, Turbulence and the dynamics of coherent structures. Parts I, II, III, *Q. Appl. Math.* **XLV**, 561–571, 573–582, 583–590 (1987).
7. L. Sirovich and H. Park, Turbulent thermal convection in a finite domain. Part I: theory, *Phys. Fluids A* **2**, 1649–1658 (1990).
8. H. Park and L. Sirovich, Turbulent thermal convection in a finite domain. Part II: numerical results, *Phys. Fluids A* **2**, 1659–1668 (1990).
9. J. L. Lumley, *Stochastic Tools in Turbulence*. Academic Press, New York (1970).
10. G. Berkooz, P. Holmes and J. L. Lumley, The proper orthogonal decomposition in the analysis of turbulent flows, *A. Rev. Fluid Mech.* **25**, 539 (1993).
11. B. A. Finlayson, *The Method of Weighted Residuals and Variational Principles*. Academic Press, New York (1972).
12. W. H. Press, S. A. Teukolsky, W. T. Vetterling and B. P. Flannery, *Numerical Recipes in Fortran: The Art of Scientific Computing*. Cambridge University Press, Cambridge (1992).